

## Analysis and Implementation of Swimming Backward for Biomimetic Carangiform Robot Fish

Chao Zhou\*, Saeid Nahavandi<sup>†</sup>, Nong Gu<sup>†</sup>, Zhiqiang Cao\*, Shuo Wang\* and Min Tan\*

\* *Laboratory of Complex Systems and Intelligence Science, Institute of Automation, Chinese Academy of Sciences, Beijing 100080, China; (e-mail: {zhouchao, zqcao, swang, tan}@compsys.ia.ac.cn).*  
<sup>†</sup> *School of Engineering and Information Technology, Deakin University, Geelong, VIC 3217, Australia; (email: {nahavand, ng}@deakin.edu.au)*

---

**Abstract:** The swimming backward for biomimetic carangiform robot fish is analyzed and implemented in this paper. The swimming law of the carangiform robot fish is modified according to the European Eel swimming mode based on the multiple-link structure to implement the backward motion. The motion mode difference between the eel and carangiform fish is discussed, and a qualitative kinematic analysis of the carangiform swimming in water is given to analyze the propulsion produced by the undulation of the multi-links tail. The experiments conducted demonstrate the good performance of the proposed method, and the results are given.

---

### 1. INTRODUCTION

The characteristics of real fishes are far better than those of ships and submarines, which attract robotics researchers greatly to develop a biomimetic robot fish with high velocity, high efficiency and high maneuverability. Many theories are proposed to explain the secrets of fish swimming mechanisms and summarize driving modes of fish motions, e.g. the elongated-body theory (M J. Lighthill, 1960, 1970), the large-amplitude elongated-body theory (M J. Lighthill, 1971), the two-dimensional (2-D) waving plate theory (T. Y. Wu, 1961) and the 3-D waving plate theory (3DWDP) (B. Tong, 2000). Generally speaking, biomimetic robot fish is defined as a fish-like aquatic vehicle based on the swimming skills and anatomic structure of a fish: the undulatory/oscillatory body motions, the highly controllable fins and the large aspect ratio lunate tail. Based on these theories, many prototypes of the biomimetic robot fish have been developed, e.g. the RoboTuna and subsequent RoboPike (M J. Lighthill, 1970, 1971), pectoral fins robot (H. Suzuki, et al. 2006), a fish-like micro robot actuated by piezoceramics (T. Fukuda, et al. 2006), The G series and MT series robot fishes (J. Liu and H. Hu, 2004), SPC series (J. Liang, et al. 2002) and CASIA-fish family (J. Yu, et al. 2004. C. Zhou, et al. 2006). Swimming backward is a special form of fish swimming in water. In nature, only European eel can swim backward by the body and tail's undulation (B. Tong, 2005), while all other fish swim backward slowly by the oscillation of pectoral fins.

Many biomimetic robots are able to swim backward. Eel-like robots are often symmetrical between the head and tail. The robot eels swim backward when the undulation amplitude of the head is larger than that of the tail. A five-link eel-like robot is developed to implement several kinds of motion including swimming backward (K. A. McIsaac and J. P. Ostrowski, 1999, 2002). Because the head link and the caudal link of the anguilliform robot fish is symmetrical, the motion

of swimming forward and backward is symmetrical and the swimming backward can be realized easily by exchanging the motion law of anterior links with the posterior ones. The structure of robot fish with ribbon fin is similar to the robot eel to a certain extent. Every fins can undulate free and symmetrical (Y. Toda, et al. 2006. M. Epstein, et al. 2006). When the anterior fins undulate larger, the robot swims backward. These two kinds of robot are both symmetrical in structure, while many other underwater robots, based on bionic fins or multiple undulation fins, utilize the fins flapping forward or backward to make the robot swim forward or backward (H. Suzuki, et al. 2006. C. Zhou, et al. 2006). All these robots have the same hydrodynamic characteristic when swimming backward and forward.

However, carangiform fish motion involves the undulation of the entire body, whose large amplitude undulation is mainly confined to the last 1/3 part of the body, which is much different from the eel. Although this difference endows the carangiform fish swim with high speed and high efficiency, the flexibility of the tail reduces and the head is not symmetrical with the tail. The carangiform robot fish has the same characteristics, so simply reverse of the motion rule is not suitable for the carangiform robot fish.

In this paper, the qualitative kinematic analysis of the carangiform swimming mode is given to discuss the propulsion. The carangiform motion is modified according to anguilliform mode to realize the swimming backward. The approach of the turning when swimming backward and emergency stop is described. The sense of the swimming backward motion for the carangiform robot fish is that it diversifies the motions without changing the mechanical structure and the advantage on propulsion, which makes the robot fish be more flexible to accomplish complex maneuverable motion in swimming. It enhances the capability and adaptability of locomotion, and simplifies the design of robot fish because the pectoral fins are needless. It

may be applied to the accurate location without large amplitude turning, the work in confined gaps, pipelines and maze etc. It enhances the capability and adaptability of locomotion and it is beyond the carangiform fish in nature at this point.

## 2. RELATIVE WORK

### 2.1 BCF mode

Lindsey studied on the BCF (Body and/or Caudal Fin) propulsion mode, and classified it as follows according to the wavelength and the amplitude envelope of the propulsive wave underlying fish's behavior.

*Anguilliform mode:* Propulsion by a muscle wave in the body of the animal progressing from head to tail like the eel, as shown in Fig.1(a), in which all or most of the body participates. The amplitude of the wave is relatively large along the whole body, and it increases toward the tail. There is at least one wavelength of the propulsive wave along the body..

*Subcarangiform mode:* As shown Fig.1 (b), it is very similar to anguilliform mode in body movement, however it amplitude of body wave is smaller and expands significantly only in the posterior half or one-third of the body.

*Carangiform mode:* For the carangiform locomotion, the body's undulations are entirely confined to the last third of the body length, and thrust is produced by means of a rather stiff caudal fin, which is shown in Fig. 1(c). Compared to anguilliform fish, carangiform swimmers are generally faster, but with less agility due to the relative rigidity of their bodies. Also, carangiform propulsion is more convenient for engineering realization.

*Thunniform mode:* Thunniform fish oscillate only a tail fin without moving the body as shown in Fig.1 (d), where thrust is generated with a lift-based method, allowing high cruising speeds to be maintained for long periods.

Most of fish swim backward by pectoral fins except European Eel, which is a kind of Anguilliform mode. The European Eel utilizes the body's undulation to swim backward.

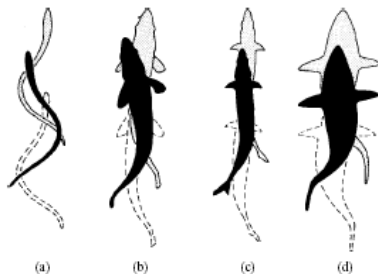


Fig. 1 The gradation of the undulatory BCF swimming

### 2.2 Carangiform Robot Fish

As described in the previous section, carangiform motion involves the undulation of the entire body, whose large amplitude undulation is mainly confined to the last 1/3 part of the body, and thrust is produced by a stiff caudal fin. The amplitude of this undulation, however, is small, or zero, in the anterior portion of the fish, increasing drastically in the immediate vicinity of the trailing edge (M. Borgen, et al. 2000). A discreted carangiform propulsive model is given to describe the motion trace of the carangiform fish spine (J. Yu, et al. 2004):

$$y_{i,j} = (c_1 x_{i,j} + c_2 x_{i,j}^2) \sin(kx_{i,j} - 2\pi i / M) \quad (1)$$

where  $y_{i,j}$  is the transverse displacement of body,  $x_{i,j}$  is the displacement along main axis,  $k$  is the body wave number ( $k = 2\pi/\lambda$ ),  $\lambda$  is the body wave length,  $c_1$  is the linear wave amplitude envelope,  $c_2$  is the quadratic wave amplitude envelope,  $\omega$  is the body wave frequency ( $\omega = 2\pi f = 2\pi/T$ ).  $i$  is the variable of spline curve sequence,  $M$  is the body-wave resolution that represents the discrete degree of the overall travelling wave, which is restricted by the maximum oscillation frequency of motors.  $j$  is the serial number of the links.

## 3. MOTION CONTROL

### 3.1 Analysis of swimming forward

We utilize multiple links tail to mimic the behaviours of carangiform fish. Once this body-wave is given, the task of the following analysis is to determine the proper body-wave constants (i.e.  $c_1, c_2, k, \omega$  etc.) for a desired swimming motion. During the swimming, the robot fish should make the links end to end on the fish body wave curve. Fig.2 shows the position of the links at a certain time. All the positions can be calculated by an iterative method (C. Zhou, 2006).

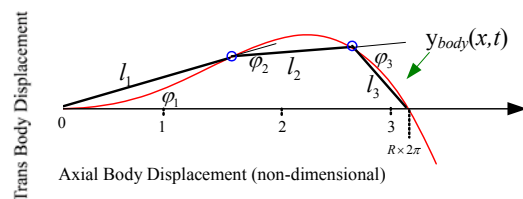


Fig. 2 Link based body-wave fitting

Swimming in water, the robot fish pushes water away behind it with using both oscillation of a tail fin and undulation of the body. This causes the fish to be propelled by the action of its body upon the water. In order to get propulsive force, the velocity of the wave should be faster than the forward speed of the fish, and amplitude of the tail part should be bigger than that of the head part. In Fig. 3, a serial curves are given to describe the positions of links at different times. In order to depict clearly, we only choose 8 curves from 18 curves during an oscillation period. These positions are calculated according to (1).

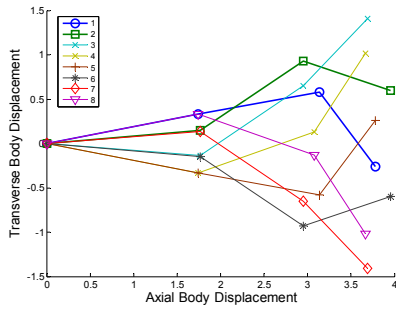


Fig. 3 An overall body-wave fitting in an oscillation cycle

No.1 and 2 curves are selected to analyze the propulsion. A fluid drag model is employed to analyze forces perpendicular to the surface of swimming robotic fish, which has been used extensively in the case of large Reynolds number in the literature [24-27], and it is:

$$F = -\mu \text{sgn}(v^\perp)(v^\perp)^2 \quad (2)$$

where  $\mu = \rho CS/2$  is the drag coefficient,  $\rho$  is the density of water,  $C$  is shape coefficient, and  $S$  is effective area.  $v^\perp$  is the projection of the velocity along the direction perpendicular to the surface.

The caudal links of the robot fish move from No.1 curve to the No.2, as shown in Fig. 4. The dynamic pressure may be calculated by (2), and the qualitative result is denoted in Fig.4

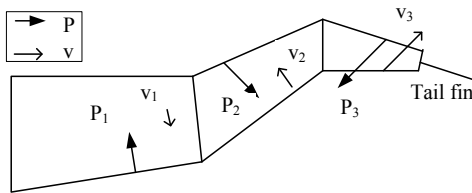


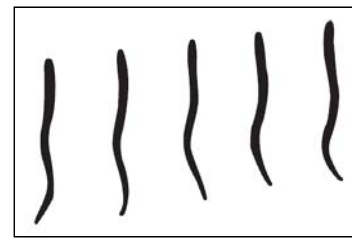
Fig.4 The dynamic pressure on the links

As shown in Fig. 4, it is the dynamic pressure distribution of robot fish body in advancing. We define the pressure which makes the robot fish moving forward as Positive pressure, and the pressure makes it swimming backward as Negative pressure. There are Positive pressure (P1, P3) and Negative pressure (P2) in Fig.4, which are all reaction force of the water. Their total force then becomes propulsive force in the axial direction of the fish body. The same analysis method can be used in a whole oscillation period. The pressure perpendicular to the axial direction is symmetrical at a motion period, and the resultant force is nearly zero. It can be found that the total Positive pressure is much greater than Negative pressure in the axial direction. That is how the three-link robot fish propel itself forward.

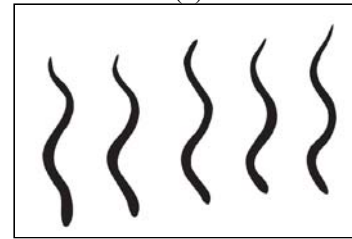
### 3.2 Method of swimming backward

The swimming forward and backward of European Eel is compared detailed in kinematics, and it is pointed out that the lateral amplitude is much higher in the rostral part of the body during backward swimming than during forward swimming, as shown in Fig. 5, and the lateral amplitude is close to that in the caudal part. (Kristiaan D'aout and Peter

Aerts, 1999)When swimming forward, the lateral amplitude in the rostral part is nearly zero.



(a)



(b)

Fig. 5. Compare of swimming forward and backward of European Eel (K. A. McIsaac and J. P. Ostrowski, 2003). (a) is the series of swimming forward and (b) is that of backward

(K. A. McIsaac and J. P. Ostrowski, 2003) gives a robot eel as an implementation of this kinematical rule, which can swim backward freely. For the carangiform robot fish, it is different from that in configuration, and a novel method should be explored to endow it with the ability to swim backward.

Base on the analysis of swimming forward, we consider that the robot fish will swim backward by making the Positive pressure be smaller than the Negative pressure in the mass in a period. According to the motion mechanism of European Eel, the amplitude of the link at forepart (the first link) should be increased. But it can not make the amplitude of the head equal to the tail, because the length of the rigid head. Thus the amplitude of the last link should be reduced. A motion curve is selected, which is similar to (1) formally with degressive envelope curve:

$$y_{i,j} = (c_1 x_{i,N+1-j} + c_2 x_{i,N+1-j}^2) \sin(kx_{i,N+1-j} - \frac{2\pi}{M} i) \quad (3)$$

where the  $N$  is the total number of links. Actually it means that the motion law of the links is reversed. The positions of links at different times in a period are drawn in Fig. 6.

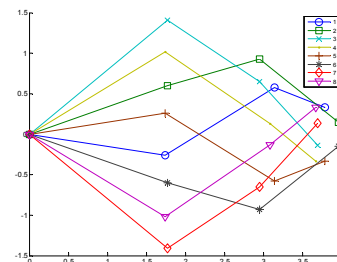


Fig. 6 The reversed body-wave fitting

In a similar way, No.1 and 2 curves are selected to analysis the propulsion and we obtain Fig. 7.

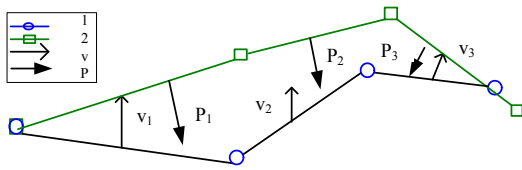


Fig. 7 The pressure analysis of reversed motion law

The change of the dynamic pressure distribution is shown in Fig.7, which are caused by increased amplitude of first link and the reduced at last link. From Fig. 7,  $P_1$  and  $P_2$  are the Negative pressure and  $P_3$  is the positive pressure. At this moment, the total pressure is Negative, which means the robot fish is propelled backward. The propulsion in the whole period can be analysed similarly and it shows that the fish may swims backward by the motion mode.

### 3.3 Other locomotion

The orientation control in advance is executed by adding different link's deflection. Different turning mode is implemented by adding various deflections  $\theta_i$ , the special deflection angles of  $j$ th link, in each oscillation period to the part or all of links. Similarly, turn in backward can be realized by the same method. Certain offset is added on every links when the law of undulation is reserved to change the axis of the oscillation. It is necessary to insure that the oscillating rule marshes the (3) when turning, so the arc is chosen as the oscillating axis of the links. Modify (3), we have:

$$y_{i,j} = (c_1 x_{i,N-j} + c_2 x_{i,N-j}^2) \sin(kx_{i,N-j} - \frac{2\pi}{M}i) + \sqrt{1/c^2 - x_{i,N-j}^2} - 1/c \quad (4)$$

where  $c$  is the curvature of the tail axis, which is connected with the turning radius.

The robot fish may achieve emergency stop during the advance with the help of swimming backward. The robot fish can switch the undulation law of every links to swimming backward mode, which will reduce the velocity quickly. This motion is useful in some situations when getting stuck in a narrow space where can not turn normally.

## 4. EXPERIMENTS

An experimental biomimetic robot fish system is constructed based on the simplified carangiform propulsive model. This robot fish is composed of a multi-link tail to fit the body wave curve and a rigid anterior part as container of control system and other accessories. (C. Zhou, et al. 2006). The experiments are conducted in an experiment pool of 1.90m\*0.95m to testify the swimming backward performance of robot fish. An overhead camera is inducted to capture the video of the robot fish motion.

The velocity is measured and it reaches the highest at the frequency of  $f=1.46\text{Hz}$ , and  $v_{\max}=5.42\text{cm/s}$ . the robot fish moves smoothly in the water when  $f<1.85\text{Hz}$ , or else it will

stagnate and become disorderly because the violent wave destroys the hydrodynamic characteristic severely at a higher frequency. When the frequency is lower than 0.74Hz, the swimming backward is too slow to measure.

The orientation control experiment is taken at the oscillation frequency of 1.63Hz. According to (4), different deflection is added to every links. The results are shown in Fig. 8.

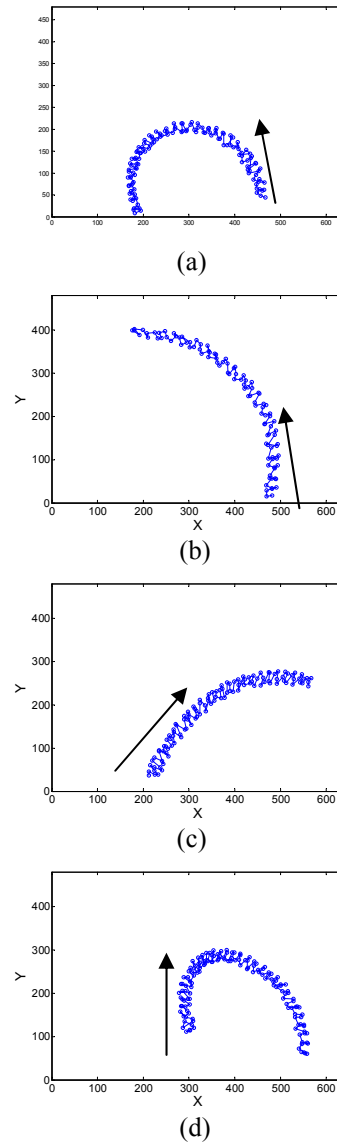


Fig. 8. Turning during swimming backward

Fig. 8 is the trace of robot fish in turning during swimming backward. The X axis and Y axis are the resolution of the video signal. The arrow is the direction of the velocity. The data in figure are the position of the fish head. These data oscillate around the trace because the shake of the fish and the error of the image recognize. The left and the right are not strictly symmetrical because the installation error of the multiple links tail.

The emergency stop experiment: The robot fish firstly swims forward by the frequency of 0.98Hz, then switch to swimming backward at  $f=1.46\text{Hz}$ . The trace is shown in Fig. 9. The forward velocity is 9.59cm/s, and the backward



velocity is 2.65 cm/s. The effect is remarkable, because the robot fish will slide for about 60cm without swimming backward.

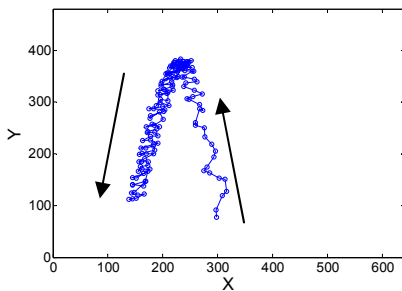


Fig. 9. Emergency stop of robot fish

## 5. CONCLUSIONS

The swimming backward motion of biomimetic carangiform robot fish is presented in this paper. Based on the biomimetic carangiform robot fish, a dynamical and kinematical analysis method is given to analyse the propulsion produced by the undulation of the multi-link tail. The difference between the anguilliform mode and carangiform mode is discussed. A method for carangiform robot fish swimming backward is proposed. Experiments verified the feasibility of the proposed method in the application of robot fish.

The future work will focus on enhancing the efficiency, agility, manoeuvrability and swimming skill based on the sensors and control technology.

## ACKNOWLEDGMENT

This work was supported in part by the National Natural Science Foundation of China (No. 60635010, No.60605026, No.60725309).

## REFERENCES

- B. Tong (2000). Propulsive mechanism of fish's undulatory motion. In: *Mechanics In Engineering*, 22: 69-74. (in Chinese)
- B. Tong, M. Sun, X. Yin (2005) A brief review on domestic research developments in biofluidynamics of animal flying and swimming," In: *Chinese Journal of Nature*. Vol.27 No.4 p191-198
- C. Zhou, L. Wang, Z. Cao, S. Wang and M. Tan (2006). The Information Processing of a Biomimetic Robot Fish Based on Multiple Sensors. *ICSCA2006*, pp.468-473
- C. Zhou, Z. Cao, S. Wang and M. Tan (2006). The Posture Control and 3-D Locomotion Implementation of Biomimetic Robot Fish. In: *IEEE IROS 2006*, pp. 5406-5411
- H. Suzuki, N. Kato, T. Katayama and Fukui Y (2006). Development of CFD-based Motion Simulator for an

- Underwater Vehicle with Mechanical Pectoral Fins. In: *ISABMEC 2006*, pp. 033
- J. Liang, T. Wang, H. Wei and W. Tao (2002). Researchful development of under water robofish II-development of a small experimental robofish. In: *Robot*. 24(3): 234-238 (in Chinese)
- J. Liu, H. Hu (2004). Building a 3D simulator for autonomous navigation of robotic fishes. In: *IEEE, IROS2004*. pp. 613 - 618
- J. Yu, M. Tan, S. Wang, E. Chen (2004). Development of a biomimetic robotic fish and its control algorithm. *IEEE Transactions on SMC*, 34 (4): 1798-1810
- K. A. McIsaac and J.P. Ostrowski(1999). A Geometric Approach to Anguilliform Locomotion: Modeling of an Underwater Eel Robot. In: *ICRA 1999*, pp. 2843-3848.
- K. A. McIsaac and J. P. Ostrowski(2003). Motion Planning for Anguilliform Locomotion. In: *IEEE Transaction on Robotics and Automation*, Vol.19, Issue 4, pp.637 – 652
- Kenneth A. McIsaac, James P. Ostrowski (1999). A Geometric Approach to Anguilliform Locomotion: Modelling with an Underwater Eel Robot. In: *ICRA1999* pp. 2843-2848
- Kenneth A. McIsaac, James P. Ostrowski (2002). Experimental verification of open-loop control for an underwater eel-like robot. In: *The International Journal of Robotics Research*. Vol. 21, iss. 10-11, pp. 849-859
- Kristiaan D'aout, Peter Aertsa(1999). Kinematic comparison of forward and backward swimming in the eel *Anguilla Anguilla*," In: *The Journal of Experimental Biology*. 202, pp. 1511-1521
- M. Borgen, G. Washington, and G. Kinzel (2000). Introducing the Carangithopter:a small piezoelectrically actuated swimming vehicle. In: *Proc. Adaptive Structures Material Systems Symp. ASME Int. Congress Exposition*, pp. 247-254.
- M. Epstein, J. E. Colgate and M. A. MacIver (2006). Generating Thrust with a Biologically-Inspired Robotic Ribbon Fin. *IEEE IROS2006*, pp. 2412 – 2417
- M J. Lighthill (1960). Note on the swimming of slender fish. In: *J. Fluid Mech*. vol.9: 305-317
- M J. Lighthill (1970). Aquatic animal propulsion of high hydromechanical efficiency. In: *J. Fluid Mech*. vol.44, 265-301
- M J. Lighthill (1971). Large-amplitude elongated-body theory of fish locomotion. In: *Proc. R. Soc. Lond, Ser. B*. vol.179, 125-138
- T. Fukuda, A. Kawamoto, F. Arai and H. Matsuura (1994). Mechanism and swimming experiment of micro mobile robot in water. In: *Proceedings, IEEE Workshop on Micro Electro Mechanical Systems*. pp273-278
- Y. Toda, H. Ikeda, and N. Sogihara (2006). The Motion of a Fish-Like Under-Water Vehicle with two Undulating Side Fins. In: *ISABMEC 2006*, pp.27
- T. Y. Wu (1961). Swimming of a waving plate. *J. Fluid Mech*. vol.10, 321-344